Materials Science Forum Vol. 753 (2013) pp 87-92

doi:10.4028/www.scientific.net/MSF.753.87

The Relationship Between Grain Boundary Energy, Grain Boundary Complexion Transitions, and Grain Size in Ca-doped Yttria

Stephanie A. Bojarski[1], Jocelyn Knighting[1], Shuailei Ma[2], William Lenthe[2], Martin P. Harmer[2], Gregory S. Rohrer[1,a]

[1]Department of Materials Science and Engineering, Carnegie Mellon University, Pittsburgh, Pennsylvania 15213, USA

[2]Department of Materials Science and Engineering, Lehigh University, Bethlehem, Pennsylvania 18015, USA

[a]rohrer@cmu.edu

Keywords: Grain boundary, grain boundary energy, complexions, thermal grooving, abnormal grain growth, yttria.

Abstract. The thermal groove technique has been used to measure relative grain boundary energies in two 100 ppm Ca-doped yttria samples. The first has a normal grain size distribution and the boundaries have a bilayer of segregated Ca. In the second sample, there is a combination of large grains and small grains. The boundaries around the large grains are known to have an intergranular film. The results show that the relative energies of boundaries in the sample with normal grain growth and the boundaries around small grains far from larger grains in the second sample are similar. Also, boundaries surrounding the largest grains and small grains immediately adjacent to them have the same and significantly lower energies. The results indicate that grain boundaries with an intergranular film have a lower energy than those with bilayer segregation and that the intergranular film extends beyond the periphery of the largest grains, but not throughout the entire sample.

Introduction

The term "complexions" refers to distinct structures and/or compositions that can occur at macroscopically identical interfaces. [1] Grain boundaries can exhibit multiple complexions; for example, an adsorbed monolayer of solute and an adsorbed bilayer of solute would be two of many possible distinct complexions that might occur at a single grain boundary. Transformations can occur from one complexion to another as a function of temperature or composition and this can be accompanied by an abrupt change in properties. [2] In other words, complexions behave in ways are that are similar to bulk phases, but are distinct because they can only exist at the interface between two different phases or two misoriented grains of the same phase. [1-8]

In at least some cases, grain boundaries with different complexions can have very different mobilities and this has a significant influence on microstructural evolution. For example, the co-existence of a high mobility and low mobility complexion in the same sample can lead to abnormal grain growth. [2] Therefore, we would like to understand what controls transitions between different grain boundary complexions. One idea is that complexion transitions occur to lower the average energy of the interface. In fact, there is growing evidence that complexion transitions are accompanied by a reduction in interface energy. Experiments on doped aluminas have shown that a complexion transition can change the relative grain boundary energy [9-10]. It has also recently been shown that the existence of a nanometer thick intergranular film reduces the energy of the Au-alumina interface. [7] Grain boundary energy measurements in Ca-doped yttria have also shown that grain boundaries in a sample with a bilayer of segregated Ca had a higher energy than grain boundaries in the same material that, after a high temperature anneal, transformed to a complexion consisting of an amorphous intergranular film. [11]

While the case for an energy reduction associated with a complexion transition is strong, there are some inconsistencies in the data reported in the earlier papers. For example, in the study of doped aluminas, Nd-, Y-, Si-, Ca-, and Mg-doped alumina all showed measurable reductions in energy when transforming from monolayer to bilayer adsorption. However, an energy decrease was not detected when the complexion transition involved an intergranular film. [9] In Ca-doped yttria, boundaries in a sample that had an intergranular film around large grains had lower energies than those with a bilayer of adsorbed Ca, but there was no difference in energy between the transformed boundaries around abnormally large grains and boundaries around small grains immediately adjacent to the large ones, which were assumed to still have the bilayer complexion. [11]

It is possible that these inconsistencies result from an assumption used in the experiments. Specifically, it was assumed that there was a sharp dividing line between transformed grain boundaries and metastable, untransformed grain boundaries and that the position of this line is marked by the boundaries of the abnormally large grains. Therefore, the measurements were conducted as illustrated schematically in Fig. 1. All comparisons were made between boundaries on the periphery of the large grains (such as between grains labeled 1 and 3 in Fig. 1) and those between smaller grains immediately adjacent to the large grain (such as between grains labeled 2 and 3 in Fig. 1). As mentioned above, in most cases there were measurable differences in energy, but there were also exceptions. The research described here was conducted to test a hypothesis that would explain the exceptional cases. Specifically, we hypothesize that the region with transformed boundaries may extend some distance beyond the large grains, so that there will be no energy difference between the boundaries around the large grain and the adjacent small grains, but that grains more distant from the abnormal grains (such as between grains labeled 4 and 5 in Fig. 1) will still have the metastable complexion and a higher relative grain boundary energy. To test this idea, we re-examined the Ca-doped yttria used in the previous work [11] and found results consistent with the hypothesis.

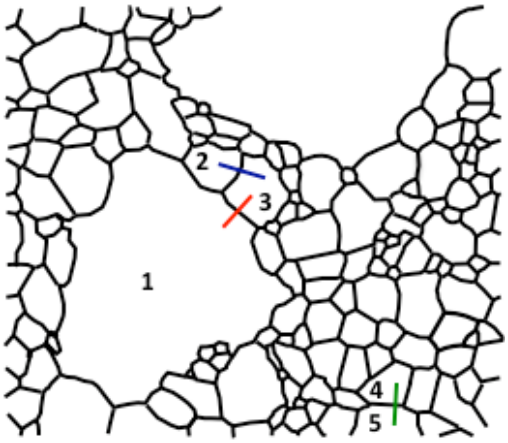

Figure 1. Schematic drawing of a microstructure with a bimodal grain size distribution, with black lines representing grain boundaries. The three types of grain boundaries are illustrated by the straight lines. The red line between 1 and 3 is a boundary on the periphery of a large grain. The blue line between grain 2 and 3 indicates a boundary between two of the smaller grains, but adjacent to a large grain. The green line between 4 and 5 indicates a boundary between two smaller grains distant from the large grains.

Experimental Procedures

The samples used in the current experiments have already been described in detail elsewhere. [11,12] Briefly, the 100 ppm Ca-doped Yttria samples were hot pressed to obtain a near theoretical density and further annealed at 1700 °C in a 5 % H_2-N_2 atmosphere with two different dwell times. The "0 hour dwell" sample was fabricated by raising the furnace temperature to 1700 °C and then immediately quenching. This sample had a normal grain size distribution and is referred to as the NGG sample. The second sample was annealed at 1700 °C for 6 h and then quenched. It had a bimodal or abnormal grain size distribution and is therefore referred to as the AGG sample.

Automated EBSD mapping was used to characterize the microstructures of the NGG and AGG samples. The EBSD step size was 0.1 μm for the NGG sample and 1 μm for the AGG sample, with orientations recorded on a hexagonal grid. The microstructures of each specimen are shown in Fig. 2. The grain size is more uniform in Fig. 2(a), labeled NGG, than in Fig. 2(b), labeled AGG.

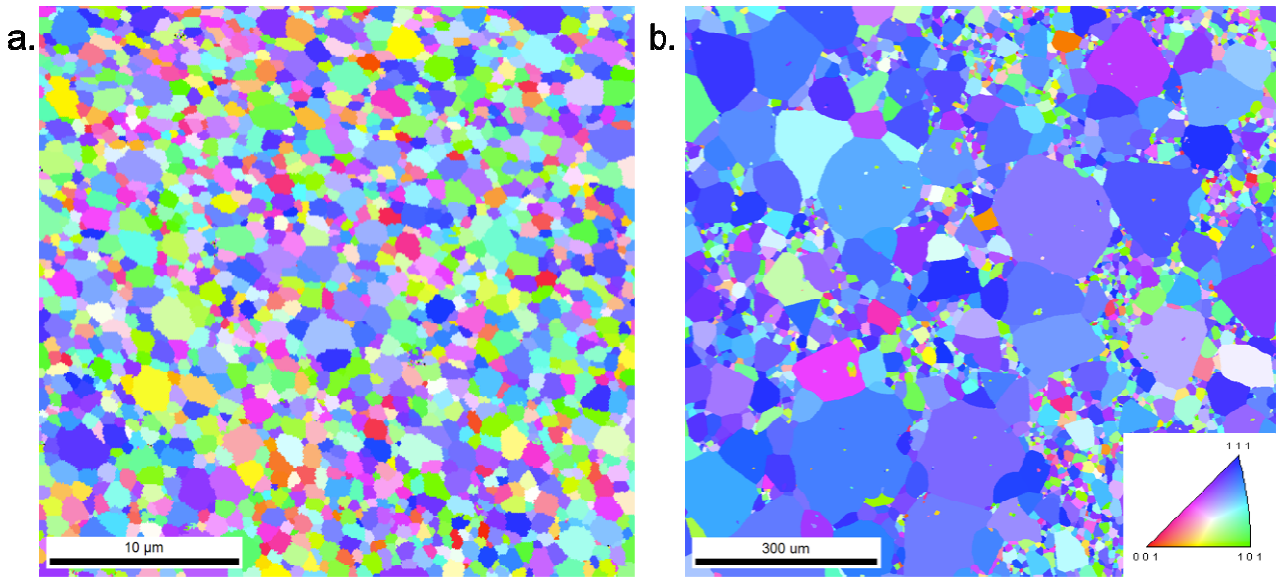

Figure 2. EBSD inverse pole figure maps of the (a) NGG and (b) AGG samples. The inset in (b) is the color code for the orientations. Note that the length scale of the AGG sample is much larger.

Thermal grooves were produced by heating the yttria samples in an air furnace (Lindberg furnace, Los Angeles, CA) for 30 min at 1300 °C; the samples were heated to this temperature at 5 °C/min and cooled at 10 °C/min. Thermal grooves form to balance the interfacial energies between the surfaces and the grain boundary. The relative energy of a grain boundary (γ_{gb}) to the adjacent grain surface (γ_s) can be expressed as a function of the dihedral angle (Ψ_s) at the groove according to equation 1.

$$\frac{\gamma_{gb}}{\gamma_s} = 2\cos\frac{\Psi_s}{2} \tag{1}$$

Using Mullins' [13] analysis it is possible to measure the height and width of a thermal groove and solve for the relative interfacial energy of the grain boundary. However, this method includes a number of approximations and assumptions. For example, it is assumed that the two surface energies are the same, that the grain boundary is normal to the surface, and that the surface energy anisotropy is small. While these assumptions will not hold for any single grain boundary, it has been found that for many measurements of grain boundary dihedral angles, the mean value and width of the distribution are reproducible and meaningful quantities. [14-16] In the last decade, atomic force microscopy (AFM) has greatly simplified these measurements and specific procedures have been established for making reliable grain boundary energy measurements using AFM. [15]

Contact AFM topographs were recorded on these grooved samples using a SolverNext NT-MDT AFM (NT-MDT, Zelenograd, Moscow) and Budget Sensor ContAL-G tips (Contact mode, R-freq=13 kHz, Force constant=0.2 N/m). The topographic images were taken with a step size of 10 nm and a 5 to 20 µm field of view. When necessary, the AFM images were edited with the open source software Gwyddion. [17] The two corrections that were sometimes applied were a plane level function to remove global tilts and, if needed, a match line correction to eliminate AFM artifacts. The dihedral angles were then determined from the widths and depths of the thermal grooves, using previously described procedures. [15]

Topographic data along lines perpendicular to grain boundaries were measured on both the NGG and AGG samples. For the NGG sample, all of the boundaries were considered equivalent. For the AGG sample, the boundaries were classified into three categories: boundaries surrounding abnormally large grains, boundaries around smaller grains that are immediately adjacent to large

grains, and boundaries around small grains that are distant (more than 10 grains removed on the plane section) from any abnormally large grains. Over 200 boundaries were measured in each group and for each one, three parallel topographic traces were extracted. A text file of thermal groove profiles was extracted using Gwyddion. [17] A program developed in house was then used to automatically determine the depth and width of the groove to calculate the dihedral angles, the relative energies, and the standard deviations of these quantities for each boundary. The accuracy of the program was verified by comparing its output to the values produced by a manual measurement.

Results

Figure 3 shows examples of topographic AFM images from which thermal groove data was extracted. The microstructure of the NGG sample is similar to undoped materials reported earlier. [18] There is one example from the NGG sample (Fig. 3(a)), the AGG sample far from an abnormally large grain (Fig. 3(b)), and the AGG sample on the periphery of a large grain (Fig. 3(c)). All images show well-formed thermal grooves, with topographic maxima (light contrast) surrounding topographic minima at the grain boundary position (dark contrast). Topographic data was obtained for lines perpendicular to boundaries with well-defined grooves in both samples.

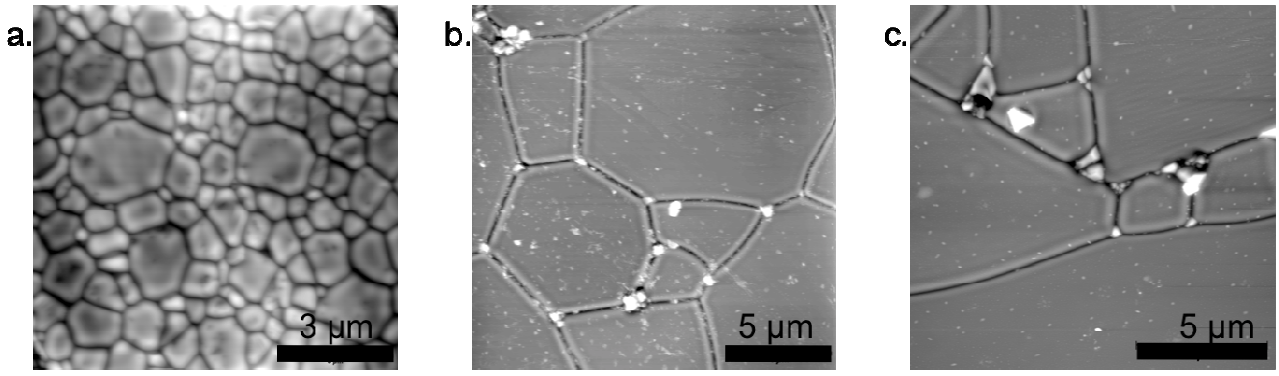

Figure 3. Topographic AFM images of the (a) NGG sample, (b) AGG sample far from abnormal grains, and (c) AGG sample with a section of a very large grain in the lower part of the field of view.

The cumulative distribution functions for the dihedral angles for the four different types of grain boundaries are shown in Fig. 4. The average values of the dihedral angle and relative interfacial energy for each boundary type are tabulated in the inset. It was found that grain boundaries in the NGG sample and around small grains distant from large ones in the AGG sample had similar dihedral angles of 155° and 152°, respectively, leading to average relative energies of 0.42 and 0.47. On the other hand, the average interfacial energy for the abnormal and normal grain boundaries adjacent to the large grains in the AGG sample is 0.28. The means that the energies of grain boundaries immediately surrounding the large grains and those adjacent to the large grains have similar energies and are at least one third lower in energy than boundaries around small grains distant from the large grains and boundaries in the NGG sample.

Discussion

The results in Fig. 4 clearly show that the grain boundaries around the very large grains and around grains adjacent to the large grains have indistinguishable energies that are lower than the others. Furthermore, the grain boundaries around small grains distant from the large ones and in the sample without abnormal grains also have similar energies that are higher. The interpretation is that both the grain boundaries around the large grains and the grains nearby have undergone a complexion transition and have an intergranular film at the boundary. The other small grains have a bilayer of Ca and, therefore, a different complexion. It should also be noted that the width of the

relative energy distribution is larger for the grains with the intergranular film. This is consistent with earlier results from doped aluminas, which showed both an increase in anisotropy and a reduction in the relative boundary energy resulting from a complexion transition. [9]

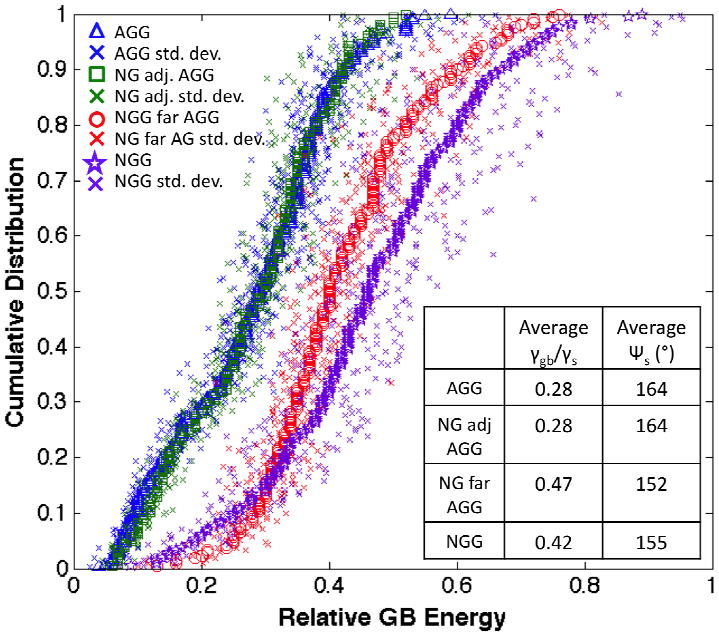

Figure 4. Cumulative distribution function comparing relative grain boundary energies for abnormal grain boundaries (triangle), normal boundaries adjacent to large grains in the AGG sample (square), normal boundaries far from large grains in the AGG sample (circle), and normal boundaries in NGG sample (star).

In the previous work on doped alumina, when the energies of boundaries around large grains were compared to the energies of boundaries around small, but adjacent grains, it was not always possible to detect a difference. One possible explanation that was suggested is that because the energy measurements are made long after the complexion transition had occurred, they do not necessarily reflect the energy at the time of the transition. Here, we propose a different explanation. The transformation of the boundary complexion occurs preferentially in boundaries connected to those that have already transformed. However, because the prior grain has a large size advantage, it rapidly annihilates the newly transformed boundary as it grows. If the complexion transition propagated faster than the growing grains, then all grains would eventually have high mobility boundaries. However, because the boundaries around the distant grains remain in a higher energy complexion, the rate of propagation must be low.

These observations provide a possible explanation for the earlier results in doped aluminas where the largest grains and the neighboring grains had the same energy. It is possible that if grains further away were probed, a decrease in energy would have been detected. It is also important to recognize that in most cases, the smaller adjacent grains did have measurably higher energies, indicating that propagation of the complexion transition beyond the first boundary does not occur in all cases. The cases where the large grains and adjacent grains had the same energy were always instances where the large grain had a complexion that involved an intergranular film. It may be that this complexion is easier to propagate than those involving ordered multilayer adsorption.

Conclusion

Measurements of the grain boundary energy in 100 ppm Ca-doped yttria indicate that boundaries around abnormally large grains and the small adjacent grains have a lower energy than small grains much further away. The higher energy grain boundaries are associated with a complexion that has a

bilayer of adsorbed Ca and the lower energy boundaries are associated a complexion that consists of an amorphous intergranular film. The measurements suggest that the intergranular film extends beyond the periphery of the largest grain, but not throughout the entire sample.

Acknowledgement

Financial support from the ONR-MURI under the grant no. N00014-11-1-0678 is gratefully acknowledged. J.K. and W.L. acknowledge the National Science Foundation – Research Experience for Undergraduates Site grant DMR-1005076.

References Cited

[1] S.J. Dillon, M. Tang, W.C. Carter, and M.P. Harmer, Complexion: A new concept for kinetic engineering in materials science, Acta Materialia, 55 (2007) 6208-6218.
[2] S.J. Dillon and M.P. Harmer, Multiple grain boundary transitions in ceramics: A case study of alumina, Acta Materialia, 55 (2007) 5247-5254.
[3] S.J. Dillon, M. P. Harmer, and J. Luo, Grain Boundary Complexions in Ceramics and Metals: An Overview, JOM, 61 (2009) 38-44.
[4] M.P. Harmer, Interfacial Kinetic Engineering: How Far Have We Come Since Kingery's Inaugural Sosman Address?, Journal of the American Ceramic Society, 93 (2010) 301-317.
[5] M. Tang, W.C. Carter, and R.M. Cannon, Diffuse interface model for structural transitions of grain boundaries, Physical Review B, 73 (2006) 14.
[6] M. Tang, W.C. Carter, and R.M. Cannon, Grain boundary transitions in binary alloys, Physical Review Letters, 97 (2006) 4.
[7] M. Baram, D. Chatain , and W.D. Kaplan, Nanometer-Thick Equilibrium Films: The Interface Between Thermodynamics and Atomistics, Science, 332 (2011) 206-209.
[8] J. Luo, H.K. Cheng, K.M. Asl, C.J. Kiely, and M. P. Harmer, The role of a bilayer interfacial phase on liquid metal embrittlement, Science, 333 (2011) 1730-1733.
[9] S.J. Dillon, M.P. Harmer, and G.S. Rohrer, The Relative Energies of Normally and Abnormally Growing Grain Boundaries in Alumina Displaying Different Complexions, Journal of the American Ceramic Society, 93 (2010) 1796-1802.
[10] S.J. Dillon, H. Miller, M.P. Harmer, and G.S. Rohrer, Grain Boundary Plane Distributions in Aluminas Evolving by Normal and Abnormal Grain Growth and Displaying Different Complexions, International Journal of Materials Research, 101 (2010) 50-56.
[11] S.A. Bojarski, S. Ma, W. Lenthe, M.P. Harmer, and G.S. Rohrer, Changes in the grain boundary character and energy distributions resulting from a complexion transition in Ca-doped Yttria, Metal. Mater. Trans A, 43A (2012) 3532-3538.
[12] S. Ma., Exploring the Role of Grain Boundary Complexions in the Sintering of Yttria Ceramics, Ph.D. Dissertation; Lehigh University, 2010.
[13] W.W. Mullins, Theory of Thermal Grooving, Journal of Applied Physics, 28 (1957) 333-339.
[14] C.A. Handwerker, J.M. Dynys, R.M. Cannon, and R.L. Coble, Dihedral Angles in Magnesia and Alumina: Distributions from Surface Thermal Grooves, Journal of the American Ceramic Society, 73 (1990) 1371-1377.
[15] D.M. Saylor and G.S. Rohrer, Measuring the Influence of Grain-Boundary Misorientation on Thermal Groove Geometry in Ceramic Polycrystals, Journal of the American Ceramic Society, 82 (1999) 1529-1536.
[16] S.J. Dillon, M.P. Harmer, and G.S. Rohrer, Influence of interface energies on solute partitioning mechanisms in doped aluminas, Acta Materialia, 58 (2010) 5097-5108.
[17] Gwyddion. http://gwyddion.net/resources.php. 2011.
[18] H. Yoshida, K. Morita, B.-N. Kim, K. Hiraga, M. Kodo, K. Soga, T. Yamamoto, Densification of Nanocrystalline Yttria by Low Temperature Spark Plasma Sintering, Journal of the American Ceramic Society, 91 (2008) 1707-10.